

Postsynthesis Modification of a Porous Coordination Polymer by LiCl To Enhance H⁺ Transport

Satoshi Horike,^{*,†,‡} Yusuke Kamitsubo,[†] Munehiro Inukai,[§] Tomohiro Fukushima,[†] Daiki Umeyama,[†] Tomoya Itakura,^{||} and Susumu Kitagawa^{*,†,§,⊥}

[†]Department of Synthetic Chemistry and Biological Chemistry, Graduate School of Engineering, Kyoto University, Katsura, Nishikyo-ku, Kyoto 615-8510, Japan

[‡]Japan Science and Technology Agency, PRESTO, 4-1-8 Honcho, Kawaguchi, Saitama 332-0012, Japan

[§]Institute for Integrated Cell-Material Sciences (WPI-iCeMS), Kyoto University, Yoshida, Sakyo-ku, Kyoto 606-8501, Japan

^{||}DENSO Corporation, 1-1 Showa-cho, Kariya, Aichi 448-8661, Japan

[⊥]Japan Science and Technology Agency, ERATO, Kitagawa Integrated Pores Project, Kyoto Research Park Bldg 3, Shimogyo-ku, Kyoto 600-8815, Japan

Supporting Information

ABSTRACT: A Ca²⁺ porous coordination polymer with 1D channels was functionalized by the postsynthesis addition of LiCl to enhance the H⁺ conductivity. The compound showed over 10⁻² S cm⁻¹ at 25 °C and 20% relative humidity. Pulse-field gradient NMR elucidated that the fast H⁺ conductivity was achieved by the support of Li⁺ ion movements in the channel.

The synthesis of solid-state proton (H⁺) conductors has been a significant challenge in many areas of chemistry.¹ In recent reports on H⁺ conductivity, crystalline coordination polymers (CPs) and metal–organic frameworks (MOFs) appear more intensively.^{2,3} Their structural versatility encourages us to design a new class of H⁺ conductors for functional materials, such as electrolytes or sensor devices. One significant target is to attain high H⁺ conductivity at ambient temperature and low relative humidity (RH).⁴ Compounds that show H⁺ conductivity >10⁻² S cm⁻¹ at room temperature and RH <30% are required for broader functional applications. However, it is difficult to create low activation energy for H⁺ conduction in solids with limited support of water molecules at ambient temperature.

To achieve high H⁺ conductivity under low RH, we require a high mobility of water molecules. Crystalline waters are not suitable because they are localized in the structures and show low mobility. One approach is the postsynthetic modification of a porous framework,^{3h,5} which could create dynamic functionality and enhance the mobility of guests. Few reports focus on the acceleration of water molecules in channels by postsynthesis treatments. Herein, we demonstrate the postsynthetic modification of a Ca²⁺-based porous CP by the inorganic salt LiCl and observe a drastic enhancement of H⁺ movement in the 1D channels. The compound showed over 10⁻² S cm⁻¹ of ion conductivity at 25 °C and RH = 20–40%. We conducted direct observations of the ion-diffusion behavior using pulse-field gradient (PFG) NMR measurements⁶ and showed that the fast H⁺ conductivity was supported by the dynamic motion of the incorporated Li⁺ ions from the LiCl.

We employed [Ca(C₄O₄)(H₂O)] (1, C₄O₄ = squarate),⁷ which has straight 1D channels with a pore diameter of 3.4 × 3.4 Å² along the *c*-axis (Figure 1a) and has one crystallo-

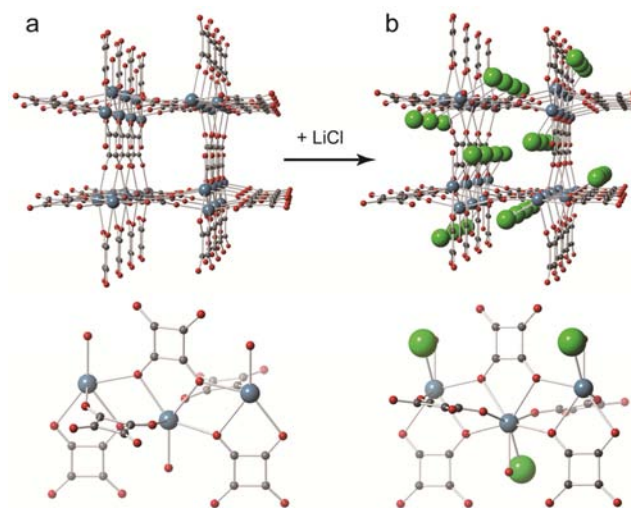


Figure 1. Crystal structures: (a) 1D_xH₂O at 10 °C (b) 1-LiCl1D_xH₂O at -50 °C along the *c*-axis (above) and the coordination environments around the Ca²⁺ ions (below). Noncoordinating waters are omitted. Blue, gray, red, and green are Ca²⁺, carbon, oxygen, and Cl⁻, respectively. For Cl⁻, one disordered position is displayed.

graphically independent Ca²⁺ ion with a seven-coordination environment. One water molecule coordinates to the Ca²⁺ center. It can adsorb the water, and we denote it as 1D_xH₂O, where *x*H₂O is the guest water molecules. At 25 °C and RH = 40%, the formula is 1D1.5H₂O, which was determined by water adsorption measurements and TGA. We evaluated the H⁺ conductivity of 1D1.5H₂O by impedance spectroscopy. The observed conductivity is negligibly low, 5.4 × 10⁻⁹ S cm⁻¹, (Figure 2) because the water molecules are strongly trapped in

Received: December 17, 2012

Published: March 14, 2013

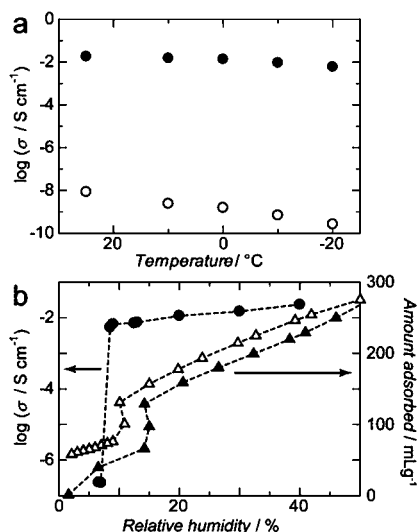


Figure 2. (a) Arrhenius plots of ion conductivity for $1\text{DxH}_2\text{O}$ (open circles) and $1\text{-LiClDxH}_2\text{O}$ (solid circles) at RH = 40%. (b) Humidity dependency of ion conductivity for $1\text{-LiClDxH}_2\text{O}$ at 25°C (solid circles). The H_2O adsorption (solid triangles) and desorption (open triangles) isotherms of 1-LiCl at 25°C .

the 1D channels and show low mobility. The low mobility was confirmed by a solid-state ^1H NMR spectrum. The framework of **1** does not contain H atoms, and the observed spectrum of ^1H represents only the water molecules. The spectrum is a characteristic doublet with peak width of 14 kHz. It is attributed to homonuclear dipole–dipole interaction and chemical shift anisotropy. The spectrum indicates that no motional averaging occurs, which suggests the low mobility of the water molecules in $1\text{D}1.5\text{H}_2\text{O}$.

To enhance the mobility of water molecules in $1\text{DxH}_2\text{O}$, we applied a postsynthetic modification. The coordinating water to the Ca^{2+} is labile, as confirmed by TGA measurement. Lithium chloride (LiCl) was reacted with $1\text{DxH}_2\text{O}$ to replace the water coordinating to the Cl^- anion (Figure 1b). LiCl is deliquescent in air, and the Cl^- would work as a ligand to the Ca^{2+} site in dissociation, while the Li^+ could interact with water molecules in the channel. The postsynthetic modification with LiCl was conducted as a solid-phase reaction in air. Powders of $1\text{DxH}_2\text{O}$ and LiCl were mechanochemically mixed by ball mill for 2 h. The sample obtained is denoted as $1\text{-LiClDxH}_2\text{O}$, and was characterized by the following analyses.

The PXRD pattern of $1\text{-LiClDxH}_2\text{O}$ does not contain the peaks of bulk LiCl. This suggests that it is not a mixture of the bulk phases of $1\text{DxH}_2\text{O}$ and LiCl. Some diffraction peaks of $1\text{-LiClDxH}_2\text{O}$ do not appear in $1\text{DxH}_2\text{O}$, which means that the crystal structure changes after the postsynthesis modification with LiCl. To characterize the crystal structure of $1\text{-LiClDxH}_2\text{O}$, single-crystal XRD was measured at -50°C . Solid-state slow reaction of $1\text{DxH}_2\text{O}$ and LiCl in air afforded rod-shaped single crystals, and the observed structure is shown in Figure 1b. In addition to the coordinating water, Cl^- ions also coordinate to the Ca^{2+} with disordering in two positions. The cell parameters of $1\text{-LiClDxH}_2\text{O}$ decrease slightly compared with those of $1\text{DxH}_2\text{O}$. The PXRD of $1\text{-LiClDxH}_2\text{O}$ matches the simulated pattern from the single-crystal structure. X-ray studies elucidated that the postsynthesis addition of LiCl to $1\text{DxH}_2\text{O}$ promoted structural modification of the overall crystal. SEM-EDX image of $1\text{-LiClDxH}_2\text{O}$ crystals showed the

homogeneous distribution of the Cl^- ions. From the crystal structure and TGA of $1\text{-LiClDxH}_2\text{O}$ and the water adsorption isotherm of 1-LiCl (Figure 2b), we concluded that the formula of $1\text{-LiClDxH}_2\text{O}$ at 25°C and RH = 40% is $[\text{Ca}(\text{C}_4\text{O}_4)(\text{Cl})_{0.5}(\text{H}_2\text{O})_{0.5}](\text{Li}_{0.5})(\text{H}_2\text{O})_{3.5}$ ($1\text{-LiClD}3.5\text{H}_2\text{O}$). The formula indicates that 1-LiCl adsorbs more water molecules per Ca^{2+} ion than **1** at the same conditions. The postsynthesis addition of LiCl provides a higher concentration of water molecules in the channels. When we tried to use other inorganic salts (LiBr, NaCl) instead of LiCl, the postsynthetic reactions with $1\text{DxH}_2\text{O}$ were not successful. This is probably because of the differences in ionic radii and the coordination strength of halogen anions.

We evaluated the mobility of ions in $1\text{-LiClD}3.5\text{H}_2\text{O}$ by solid-state NMR spectrum. The ^1H spectrum under static condition showed a sharp single peak at 5 ppm, which is obviously different from that of $1\text{D}1.5\text{H}_2\text{O}$. This indicates that the water molecules in $1\text{-LiClD}3.5\text{H}_2\text{O}$ move more freely. We also measured the solid-state ^7Li NMR under the static condition. Only a sharp single peak was observed, which suggests the liquid-like fast motion of the lithium species. We then investigated the ion conductivity of $1\text{-LiClD}3.5\text{H}_2\text{O}$ (Figure 2a). A significant increase in the bulk ionic conductivity was observed and was $1.8 \times 10^{-2} \text{ S cm}^{-1}$ at 25°C and RH = 40%. At this stage, we cannot claim that the main contribution of the ion conductivity was from H^+ , because the Li^+ ions also move quickly according to the NMR results. The mechanism is discussed later. We measured the temperature dependency of the conductivity of $1\text{-LiClDxH}_2\text{O}$ from 25 to -20°C . The estimated activation energy of the ion conductivity of $1\text{-LiClDxH}_2\text{O}$ from an Arrhenius plot is low (0.18 eV), which is in the range of Grotthus-type H^+ transfer.^{1b} Even at -20°C and RH = 40%, where the relative pressure of water is 0.13 kPa, the high ion conductivity is retained ($8 \times 10^{-3} \text{ S cm}^{-1}$). Meanwhile, the activation energy of the H^+ conductivity of **1** is 0.46 eV. Compared with $1\text{DxH}_2\text{O}$, $1\text{-LiClDxH}_2\text{O}$ shows $>10^6$ times greater conductivity. There are also several reports on Ca^{2+} based coordination polymers with H^+ conductivity under humid conditions.⁸ A relatively large ionic radius of Ca^{2+} would work for high H^+ conductivity.

To elucidate the ion conduction behavior in the 1D channels, we measured PFG NMR for both ^1H and ^7Li of $1\text{-LiClD}3.5\text{H}_2\text{O}$. PFG NMR can monitor the displacement of NMR-active nuclei inside the channel. The spin–echo intensity ($I/I_0(b) = \exp(-D \times b)$) of $1\text{-LiClD}3.5\text{H}_2\text{O}$ was observed as a function of the parameter $b = (\gamma\delta G)^2(\Delta/3 - \delta/9)$, as shown in Figure 3.⁹ The slopes of these decays represent self-diffusion coefficients D . Considering the narrow 1D channel of the crystal structure, we can approximate that the decay of spin–echo intensities is caused by the diffusion of ^1H and ^7Li along the channel. Based on the model of 1D diffusion,⁹ the obtained D of ^1H is $6.1 \times 10^{-10} \text{ m}^2 \text{ s}^{-1}$. The $D(^1\text{H})$ and H^+ conductivity of $1\text{-LiClD}3.5\text{H}_2\text{O}$ are similar to those of Nafion 117, which is a popular H^+ conductor ($D(^1\text{H}) = 8.0 \times 10^{-10} \text{ m}^2 \text{ s}^{-1}$ and conductivity is $1.4 \times 10^{-3} \text{ S cm}^{-1}$ at 31°C and RH = 40%).¹⁰ This indicates that fast, long-range H^+ hopping occurs in the 1D channel. Interestingly, the observed $D(^7\text{Li})$ is $4.9 \times 10^{-10} \text{ m}^2 \text{ s}^{-1}$, which is comparable with that of H^+ . This indicates that the Li^+ also shows the fast diffusion in the channel. From the Nyquist plot of $1\text{-LiClD}3.5\text{H}_2\text{O}$, we could not distinguish the H^+ and Li^+ conductivities. The study of the diffusion coefficients of ^1H and ^7Li indicates that both H^+ and Li^+ have high mobility in the channel. We consider that the Li^+ ions

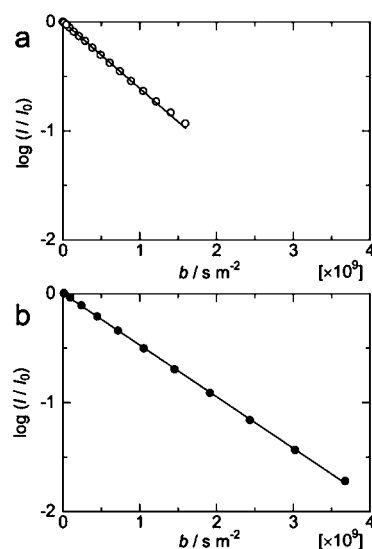


Figure 3. Spin-echo attenuation in PFG NMR spectra for: (a) ^1H and (b) ^7Li in $1\text{-LiCl}\cdot 3.5\text{H}_2\text{O}$ at $25\text{ }^\circ\text{C}$ and $\text{RH} = 40\%$.

mutually interact with the H^+ from the water molecules, and the diffusive motion of Li^+ would contribute to the enhancement of conductivity of H^+ in the channel. The postsynthesis addition of LiCl to the unsaturated open metal sites via the coordination bond could change the chemical environment of the pores. It consequently enhances the concentration and dynamics of water molecules in the pores.

To confirm the H^+ transport in $1\text{-LiCl}\cdot x\text{H}_2\text{O}$ and its function as a solid electrolyte at low RH, we fabricated a membrane-electrode assembly, and the electromotive force of the dry H_2/air cell was measured at $23\text{ }^\circ\text{C}$ and $\text{RH} = 20\%$. The observed open-circuit voltage is $\sim 1.0\text{ V}$, which is sufficiently high compared with the theoretical value under these conditions (1.18 V). The value was retained for over 2 h. This indicates that the H^+ can transport through the pellet of $1\text{-LiCl}\cdot x\text{H}_2\text{O}$ and that there is no considerable fuel gas permeability to decrease the voltage in these conditions.

We checked the dependence of ion conductivity of $1\text{-LiCl}\cdot x\text{H}_2\text{O}$ on the RH and the water adsorption/desorption isotherms of 1-LiCl at $25\text{ }^\circ\text{C}$ (Figure 2b). As the RH decreases from 40%, the observed ion conductivity decreases slightly. Even at $\text{RH} = 10\%$, the ion conductivity of $1\text{-LiCl}\cdot x\text{H}_2\text{O}$ remains high ($9.0 \times 10^{-3}\text{ S cm}^{-1}$). This is because the accommodated water molecules are not released from the pores. In the desorption profile of water, a hysteresis is observed which indicates the relatively strong interaction with host framework, and a sudden decrease of the uptake amount is observed at $\text{RH} = 10\%$. This suggests that $1\text{-LiCl}\cdot x\text{H}_2\text{O}$ could hold sufficient water molecules even around $\text{RH} = 10\%$ and abruptly releases them below $\text{RH} = 10\%$. Indeed, the observed ion conductivity significantly decreases at $\text{RH} = 9\%$ ($2.5 \times 10^{-7}\text{ S cm}^{-1}$ at $25\text{ }^\circ\text{C}$). This is because of the low mobility and concentration of the water molecules. The incorporated Li^+ in the channel could not enhance the conductivity at this condition. The ^7Li NMR spectrum of $1\text{-LiCl}\cdot x\text{H}_2\text{O}$ below $\text{RH} = 10\%$ showed a broad pattern that suggests the deceleration of the motion of Li^+ ions.

In conclusion, we have demonstrated high H^+ conductivity by use of the microporous coordination polymer $[\text{Ca}(\text{C}_4\text{O}_4)]$ (**1**, $\text{C}_4\text{O}_4 = \text{squarate}$) with its pores functionalized by LiCl via postsynthetic modification. The compound has conductivities

of $1.8 \times 10^{-2}\text{ S cm}^{-1}$ at $25\text{ }^\circ\text{C}$ and $\text{RH} = 40\%$ and $9.0 \times 10^{-3}\text{ S cm}^{-1}$ at $\text{RH} = 10\%$. The conductivity at low RH and at room temperature is considerably high among the reported coordination polymers³¹ and other compounds. We also confirmed its electrolyte performance by monitoring the open-circuit voltage of an H_2/air cell at $25\text{ }^\circ\text{C}$ and $\text{RH} = 20\%$. Solid-state NMR elucidated that the high H^+ conductivity is assisted by the movement of Li^+ species in the 1D channels. The postsynthesis modification of the pore surface of CPs/MOFs is regarded as a powerful approach to enhance the dynamics and to increase the concentration of water molecules, resulting in high H^+ conductivity under low RH.

■ ASSOCIATED CONTENT

Supporting Information

Sample preparations, TGA curves, PXRDs, elemental analyses, H_2O adsorption/desorption isotherms, impedance spectroscopies, solid-state NMR spectra, SEM-EDX images. This material is available free of charge via the Internet at <http://pubs.acs.org>.

■ AUTHOR INFORMATION

Corresponding Authors

horike@sbchem.kyoto-u.ac.jp; kitagawa@icems.kyoto-u.ac.jp

Notes

The authors declare no competing financial interest.

■ ACKNOWLEDGMENTS

This work was supported by the Japan Science and Technology Agency PRESTO program, Grants-in-Aid for Scientific Research, the Japan Society for the Promotion of Science (JSPS) and the Japan Science and Technology Agency ERATO program. iCeMS is supported by the World Premier International Research Initiative (WPI), MEXT, Japan.

■ REFERENCES

- (1) (a) Kudo, T.; Fueki, K. *Solid State Ionics*; Wiley: Hoboken, 1990 (b) Colombari, P. *Proton conductors; Solids, membranes and gels-materials and devices*; Cambridge University Press: Cambridge, 1992 (c) Li, Q. F.; He, R. H.; Jensen, J. O.; Bjerrum, N. J. *Chem. Mater.* **2003**, *15*, 4896. (d) Kreuer, K. D.; Paddison, S. J.; Spohr, E.; Schuster, M. *Chem. Rev.* **2004**, *104*, 4637. (e) Norby, T.; Wideroe, M.; Glockner, R.; Larring, Y. *Dalton Trans.* **2004**, 3012. (f) Imai, H.; Akutagawa, T.; Kudo, F.; Ito, M.; Toyoda, K.; Noro, S.; Cronin, L.; Nakamura, T. *J. Am. Chem. Soc.* **2009**, *131*, 13578. (g) Laberty-Robert, C.; Valle, K.; Pereira, F.; Sanchez, C. *Chem. Soc. Rev.* **2011**, *40*, 961. (h) Tolle, P.; Kohler, C.; Marschall, R.; Sharifi, M.; Wark, M.; Frauenheim, T. *Chem. Soc. Rev.* **2012**, *41*, 5143.
- (2) (a) Yaghi, O. M.; Li, H. L.; Davis, C.; Richardson, D.; Groy, T. L. *Acc. Chem. Res.* **1998**, *31*, 474. (b) Cheetham, A. K.; Férey, G.; Loiseau, T. *Angew. Chem., Int. Ed.* **1999**, *38*, 3268. (c) Kitagawa, S.; Kitaura, R.; Noro, S. *Angew. Chem., Int. Ed.* **2004**, *43*, 2334. (d) Férey, G. *Chem. Soc. Rev.* **2008**, *37*, 191. (e) Chen, B. L.; Xiang, S. C.; Qian, G. D. *Acc. Chem. Res.* **2010**, *43*, 1115. (f) D'Alessandro, D. M.; Smit, B.; Long, J. R. *Angew. Chem., Int. Ed.* **2010**, *49*, 6058. (g) Farha, O. K.; Hupp, J. T. *Acc. Chem. Res.* **2010**, *43*, 1166. (h) Della Rocca, J.; Liu, D. M.; Lin, W. B. *Acc. Chem. Res.* **2011**, *44*, 957. (i) Zhou, H. C.; Long, J. R.; Yaghi, O. M. *Chem. Rev.* **2012**, *112*, 673. (j) Wu, H. H.; Gong, Q. H.; Olson, D. H.; Li, J. *Chem. Rev.* **2012**, *112*, 836. (k) Miras, H. N.; Yan, J.; Long, D. L.; Cronin, L. *Chem. Soc. Rev.* **2012**, *41*, 7403.
- (3) (a) Kitagawa, H.; Nagao, Y.; Fujishima, M.; Ikeda, R.; Kanda, S. *Inorg. Chem. Commun.* **2003**, *6*, 346. (b) Bureekaew, S.; Horike, S.; Higuchi, M.; Mizuno, M.; Kawamura, T.; Tanaka, D.; Yanai, N.; Kitagawa, S. *Nat. Mater.* **2009**, *8*, 831. (c) Hurd, J. A.; Vaidyanathan, R.; Thangadurai, V.; Ratcliffe, C. I.; Moudrakovski, I. L.; Shimizu, G. K.

- Nat. Chem.* **2009**, *1*, 705. (d) Yamada, T.; Sadakiyo, M.; Kitagawa, H. *J. Am. Chem. Soc.* **2009**, *131*, 3144. (e) Ohkoshi, S.; Nakagawa, K.; Tomono, K.; Imoto, K.; Tsunobuchi, Y.; Tokoro, H. *J. Am. Chem. Soc.* **2010**, *132*, 6620. (f) Taylor, J. M.; Mah, R. K.; Moudrakovski, I. L.; Ratcliffe, C. I.; Vaidhyanathan, R.; Shimizu, G. K. H. *J. Am. Chem. Soc.* **2010**, *132*, 14055. (g) Pardo, E.; Train, C.; Gontard, G.; Boubekeur, K.; Fabelo, O.; Liu, H.; Dkhil, B.; Lloret, F.; Nakagawa, K.; Tokoro, H.; Ohkoshi, S.; Verdaguer, M. *J. Am. Chem. Soc.* **2011**, *133*, 15328. (h) Wiers, B. M.; Foo, M. L.; Balsara, N. P.; Long, J. R. *J. Am. Chem. Soc.* **2011**, *133*, 14522. (i) Panda, T.; Kundu, T.; Banerjee, R. *Chem. Commun.* **2012**, *48*, 5464. (j) Umeyama, D.; Horike, S.; Inukai, M.; Itakura, T.; Kitagawa, S. *J. Am. Chem. Soc.* **2012**, *134*, 12780. (k) Ponomareva, V. G.; Kovalenko, K. A.; Chupakhin, A. P.; Dybtsev, D. N.; Shutova, E. S.; Fedin, V. P. *J. Am. Chem. Soc.* **2012**, *134*, 15640. (l) Yoon, M.; Suh, K.; Natarajan, S.; Kim, K. *Angew. Chem., Int. Ed.* **2013**, *52*, 2688.
- (4) (a) Daiko, Y.; Kasuga, T.; Nogami, M. *Chem. Mater.* **2002**, *14*, 4624. (b) Moghaddam, S.; Pengwang, E.; Jiang, Y. B.; Garcia, A. R.; Burnett, D. J.; Brinker, C. J.; Masel, R. I.; Shannon, M. A. *Nanotechnol.* **2010**, *5*, 230. (c) Sadakiyo, M.; Okawa, H.; Shigematsu, A.; Ohba, M.; Yamada, T.; Kitagawa, H. *J. Am. Chem. Soc.* **2012**, *134*, 5472.
- (5) (a) Wang, Z.; Cohen, S. M. *J. Am. Chem. Soc.* **2007**, *129*, 12368. (b) Burrows, A. D.; Frost, C. G.; Mahon, M. F.; Richardson, C. *Angew. Chem., Int. Ed.* **2008**, *47*, 8482. (c) Cohen, S. M. *Chem. Rev.* **2012**, *112*, 970. (d) Valtchev, V.; Majano, G.; Mintova, S.; Perez-Ramirez, J. *Chem. Soc. Rev.* **2012**.
- (6) Kärger, J.; Ruthven, D. M. *Diffusion in Zeolites and Other Microporous Solids*; Wiley: Hoboken, 1992.
- (7) Robl, C.; Weiss, A. *Mater. Res. Bull.* **1987**, *22*, 373.
- (8) (a) Mallick, A.; Kundu, T.; Banerjee, R. *Chem. Commun.* **2012**, *48*, 8829. (b) Kundu, T.; Sahoo, S. C.; Banerjee, R. *Chem. Commun.* **2012**, *48*, 4998.
- (9) (a) Callaghan, P. T.; Jolley, K. W.; Lelievre, J. *Biophys. J.* **1979**, *28*, 133. (b) Callaghan, P. T.; Soderman, O. *J. Phys. Chem.* **1983**, *87*, 1737.
- (10) Ochi, S.; Kamishima, O.; Mizusaki, J.; Kawamura, J. *Solid State Ionics* **2009**, *180*, 580.